Chemistry - A European Journal 23.36 (2017): 8623-8627
DOI: https://doi.org/10.1002/chem.201702072

Electronic Supporting Information

Confining functional nanoparticles into colloidal imine-based COF spheres by a sequential encapsulation-crystallization method

David Rodríguez-San-Miguel, Amirali Yazdi, Vincent Guillerm, Javier Pérez-Carvajal, Víctor Puntes, Daniel Maspoch and Félix Zamora

MATERIALS AND METHODS

1,3,5-benzenetricarboxaldehyde (BTCA) was obtained from Manchester Organics. 1,3,5-tris-(4'-aminophenyl)benzene (TAPB) was prepared according to literature procedures.[1] Other chemicals and solvents were obtained from Sigma-Aldrich and used without further purification unless specified.

Attenuated Total Reflection Fourier Transform Infrared Spectroscopy: ATR-FT-IR spectroscopy was recorded in a Perkin Elmer Spectrum 100 with a PIKE Technologies MIRacle Single Reflection Horizontal ATR accesory with a spectral range of 4000-650 cm^{-1}.

Solid-State ^{13}C CP-MAS Nuclear Magnetic Resonance Spectroscopy. Solid-state nuclear magnetic resonance (NMR) spectra were recorded at room temperature on a Bruker AV 400 WB spectrometer using a triple channel 4 mm probe with zirconia rotors and a Kel-F cap. Cross-polarization with MAS (CP-MAS) was used to acquire ^{13}C data at 100.61 MHz. The spectral width of the pulse sequence was 35 kHz. The ^{1}H excitation pulse was 3 μs. The CP contact time was 3.5 ms. High power two-pulse phase modulation (TPPM) ^{1}H decoupling was applied during data acquisition using a decoupling frequency of 80 kHz. Recycle delays were 4 s. The sample spinning rate was 10 kHz.

Thermogravimetry. Thermogravimetric analyses of samples were run on a Thermobalance TGA Q-500 thermal gravimetric analyzer with samples held in a platinum pan under nitrogen atmosphere. A 10 K min^{-1} ramp rate was used.

Elemental Analysis: Elemental analyses were obtained using LECO CHNS-932 elemental analyzer.

Field-Emission Scanning Electron Microscopy: Field-emission scanning electron microscopy (FE-SEM) images were collected on a scanning electron microscope (FEI Magellan 400L XHR) at an acceleration voltage of 1.0 kV, using aluminium as a support.

Transmission Electron Microscopy: High-Angle Annular Dark-Field Scanning Transmission Electron Microscopy (HAADF-STEM) and TEM images and Energy Dispersive X-ray Spectroscopy (EDX) composition profiles were collected on a Transmission Electron Microscope FEI Tecnai G2 F20 at 200 kV.

Powder X-Ray Diffraction: Powder X-ray diffraction (PXRD) data were collected at 100 K at XALOC beamLine at ALBA synchrotron[2] (λ = 0.82653 Å). Data were integrated and scaled using the Fit2D program.[3]

Inductively Coupled Plasma - Mass Spectrometry: ICP-MS measurements were performed using an ICP-MS Agilent Series 7500.

Gas Adsorption: Volumetric N_2 and CO_2 sorption isotherms were collected at 77 K (N_2) and 203 K, 258 K, 273 K, 288 K, 298 K (CO_2) using an ASAP 2020 HD (Micromeritics). Temperature was controlled by a liquid nitrogen bath (77 K) or Lauda Proline RP 890 chiller (203 K – 298 K). As recommended by Rouquerol (COPS X conference, Characterization Of Porous Solids, Granada, 2014), Brunner Emmet Teller (BET) area and total pore volumes are selected preferentially to Langmuir model for the evaluation and comparison of the porosity of MOFs. BET areas (A_{BET}) were calculated using MicroActive software within an appropriate pressure range in order to keep the C constant positive, using the criteria recommended by Rouquerol *et al*.[4] The micropore volumes (V_μ) were calculated at

$P/P_0 = 0.3$, whereas the total pore volumes (V_t) were calculated at $P/P_0 = 0.95$. Samples were outgassed for 12 h under secondary vacuum at 150ºC.

UV−Visible Spectroscopy: UV−visible spectra were acquired with a Shimadzu UV- 2400 spectrophotometer. Samples were placed in a cell, and spectral analysis was performed at room temperature.

Dynamic Light Scattering: Dynamic light scattering (DLS) spectra were acquired with a Zetasizer Nano ZS. Samples were dispersed in water and placed in a cell, and spectral analysis was performed at room temperature.

SYNTHETIC PROCEDURES

a-1 Spheres: BTCA (46 mg, 0. 28 mmol) was dissolved in 15 mL of acetone and 3 mL of acetic acid. Separately, TAPB (100 mg, 0.28 mmol) was also dissolved in 15 mL of acetone. The resulting solutions were mixed and stirred for 1 h. A turbid yellow suspension was formed. The reaction mixture was centrifuged at 18407 rcf for 2 min. The supernatant was removed and the yellow solid was washed twice with 20 mL of acetone and twice with 20 mL of tetrahydrofuran (THF), isolating it by means of centrifugation at 18407 rcf for 2 min. Finally, the solid was allowed to dry in ambient conditions for 48 h and under vacuum at 150 ºC for 24 h to produce 116 mg (85 % yield) of yellow powder. Elemental analysis calculated for $C_{33}H_{21}N_3 \cdot H_2O$: C: 83.02 %; H: 4.82 %; N: 8.81 %. Found: C: 82.97 %; H: 4.88 %; N: 8.56 %.

c-1 Spheres: **a-1** (116 mg) was dispersed in a mixture of 10.5 mL of 1,4-dioxane, 2.1 mL of mesitylene, 2.1 mL of water and 3.1 mL of acetic acid and heated for 7 days. After cooling, the mixture was centrifuged at 2348 rcf for 3 min. The supernatant was removed and the yellow solid was washed with toluene (20 + 12 mL), isolating it by means of centrifugation at 2348 rcf for 3 min. Finally, the solid was allowed to dry in ambient conditions for 48 h and under vacuum at 150 ºC for 24 h to produce 112 mg (97 % yield) of yellow powder. Elemental analysis calculated for $C_{33}H_{21}N_3 \cdot H_2O$: C: 83.02 %; H: 4.82 %; N: 8.81 %. Found: C: 83.20 %; H: 4.91 %; N: 8.22 %.

PVP Stabilized Gold Nanoparticles*:* A solution of 2.2 mM sodium citrate in Milli-Q water (150 mL) was heated with a heating mantle in a 250 mL three-necked round-bottomed flask for 15 min under vigorous stirring. A condenser was utilized to prevent the evaporation of the solvent. After boiling had commenced, 1 mL of $HAuCl_4$ (25 mM) was injected. The colour of the solution changed from yellow to bluish gray and then, to soft pink in 10 min. Under these conditions, the resulting particles (9 ± 2.4 nm, ∼3×10^{12} NPs/mL) were coated with negatively charged citrate ions and hence, they were well suspended in H_2O. After the gold nanoparticle solution was cooled to room temperature, a solution of 0.5 g poly (vinylpyrrolidone) (PVP, MW = 40,000) in water (20 mL) was added dropwise to the gold nanoparticle solution under continuous stirring, and the mixture was further stirred at room temperature for 24 h. Then, 600 mL of acetone were added to this mixture and left overnight. The supernatant was removed, and the resulting nanoparticles were washed one time with methanol and twice with acetone, and finally dispersed in 10 mL of acetone at a concentration of 0.6 $mg.mL^{-1}$.[5]

PVP Stabilized Palladium Nanoparticles*:* Na_2PdCl_4 (44 mg) was dissolved in 20 mL of ethylene glycol in the presence of 222 mg of poly (vinylpyrrolidone) (PVP, MW = 55,000) in a three-neck round-bottomed flask. This solution was heated up to 180 °C for 10 min and, after cooling down to room temperature, 150 mL of acetone was added to the as-synthesized PVP stabilized palladium

nanoparticles. Then, the precipitated nanoparticles were dispersed in ethanol, washed twice with ethanol and once with acetone, and finally redispersed in acetone to give a colloidal solution of palladium nanoparticles at a concentration of 0.5 mg.mL^{-1}. The average size of the palladium nanoparticles was 3.3 ± 1.1 nm.

PVP Stabilized Iron Oxide Nanoparticles*:* Iron oxide magnetic nanoparticles were prepared by the conventional co-precipitation method. 4 g of $FeCl_3.6H_2O$, 1.25 g of $FeCl_2.4H_2O$ and 300 mg of poly (vinylpyrrolidone) (PVP, MW = 55,000) were dissolved in 50 mL of Milli-Q water under nitrogen under vigorous stirring at 80˚ C. Then, 0.5 mL of NH_4OH (15 M) was added and the solution was heated for another 1.5 h. After cooling, the nanoparticles were sequentially washed with Milli-Q water and ethanol several times. Finally, nanoparticles were washed twice with acetone and the cleaned nanoparticles were dispersed in acetone at a concentration of 1 mg. mL^{-1}.[6] The average size of the iron oxide nanoparticles was 9.8 ± 3.9 nm.

Au@c-1 Spheres: BTCA (20 mg, 0.12 mmol) was dissolved in 1.33 mL of gold nanoparticle suspension, 5.33 mL of acetone and 1.33 mL of acetic acid. Separately, TAPB (43 mg, 0.12 mmol) was also dissolved in 1.33 mL of gold nanoparticle suspension and 5.33 mL of acetone. The resulting solutions were mixed and stirred for 1 h. A pink precipitate was formed in a turbid salmon suspension. The reaction mixture was centrifuged at 24 rcf for 5 min. The turbid salmon supernatant was removed and the pink solid was washed twice with 9 mL of acetone and twice with 9 mL of THF, isolating it by means of centrifugation for 5 min at 94 rcf. The solid was dispersed in a mixture of 5.25 mL of 1,4-dioxane, 1.05 mL of mesitylene, 1.05 mL of water and 1.56 mL of acetic acid and heated for 7 days. After cooling, the mixture was centrifuged at 2348 rcf for 3 min. The supernatant was removed and the solid was washed with thrice with 6 mL of toluene, isolating it by means of centrifugation at 2348 rcf for 3 min. Finally, the solid was allowed to dry in ambient conditions for 48 h and under vacuum at 80 ºC for 24 h to produce 8.5 mg of brownish-pink powder.

Pd@c-1 Spheres: BTCA (20 mg, 0.12 mmol) was dissolved in 1.33 mL of palladium nanoparticle suspension, 5.33 mL of acetone and 1.33 mL of acetic acid. Separately, TAPB (43 mg, 0.12 mmol) was also dissolved in 1.33 mL of palladium nanoparticle suspension and 5.33 mL of acetone. The resulting solutions were mixed and stirred for 1 h. A black precipitate was formed in a turbid yellow suspension. The reaction mixture was centrifuged at 24 rcf for 5 min. The turbid yellow supernatant was removed and the black solid was washed twice with 9 mL of acetone and twice with 9 mL of THF, isolating it by means of centrifugation for 5 min at 94 rcf. The solid was dispersed in a mixture of 5.25 mL of 1,4-dioxane, 1.05 mL of mesitylene, 1.05 mL of water and 1.56 mL of acetic acid and heated for 7 days. After cooling, the mixture was centrifuged at 2348 rcf for 3 min. The supernatant was removed and the yellow solid was washed with thrice with 6 mL of toluene, isolating it by means of centrifugation at 2348 rcf for 3 min. Finally, the solid was allowed to dry in ambient conditions for 48 h and under vacuum at 80 ºC for 24 h to produce 10 mg of yellow powder.

Fe_3O_4@c-1 Spheres: BTCA (150 mg, 0.93 mmol) was dissolved in 25 mL of iron oxide nanoparticle suspension, 25 mL of acetone and 10 mL of acetic acid. Separately, TAPB (325 mg, 0.93 mmol) was also dissolved in 25 mL of iron oxide nanoparticle suspension and 25 mL of acetone. The resulting solutions were mixed and ultrasonicated for 1 h. A brown precipitate was formed in a turbid yellow suspension. The turbid yellow supernatant was removed by means of magnetic decantation. The brown solid was washed thrice with 30 mL of acetone and twice with 30 mL of THF. The solid was dispersed in a mixture of 34.25 mL of 1,4-dioxane, 6.85 mL of mesitylene, 6.85 mL of water and 10.2 mL of acetic acid and heated for 7 days. After cooling, the supernatant was removed by means of magnetic decantation and the solid was washed once with 25 mL of ethanol and twice with 20 mL of toluene.

Finally, the solid was allowed to dry in ambient conditions for 48 h and afterwards was dried under vacuum at 80 ºC for 24 h to produce 142 mg of a yellow powder.

4-nitrophenol (4-NP) Reduction*:* The catalytic reactions were conducted by mixing 0.5 mL of an aqueous solution of $NaBH_4$ (1.3 M) with 3.0 mL of an aqueous solution of 4-NP (0.125 mM). After 2 min, 0.2 mL of an aqueous solution of 0.15 mg·mL^{-1} of **Pd@a-1/Pd@c-1** or 0.4 mL of an aqueous solution of 0.15 mg·mL^{-1} of **Au@a-1/Au@c-1** were injected into the reaction mixture. The catalytic reaction was then followed every 2 min by UV−vis spectroscopy in the range of 280−460 nm.

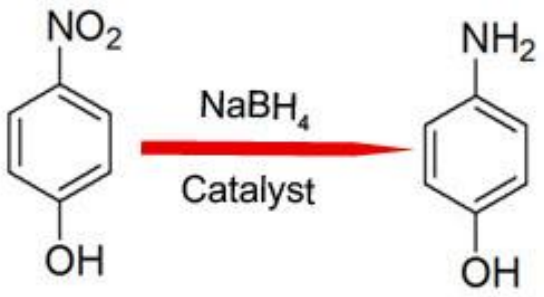

CHARACTERIZATION

Figure S1. ATR-FT-IR spectra of monomers **BTCA** (red) and **TAPB** (blue), of **a-1** (orange) and of **c-1** (green). The most significant changes are highlighted: Disappearance of N-H stretching bands between 3300-3500 cm^{-1}, decrease of the intensity of C=O stretching band at 1689 cm^{-1}, and appearance of C=N stretching band at 1623 cm^{-1}.

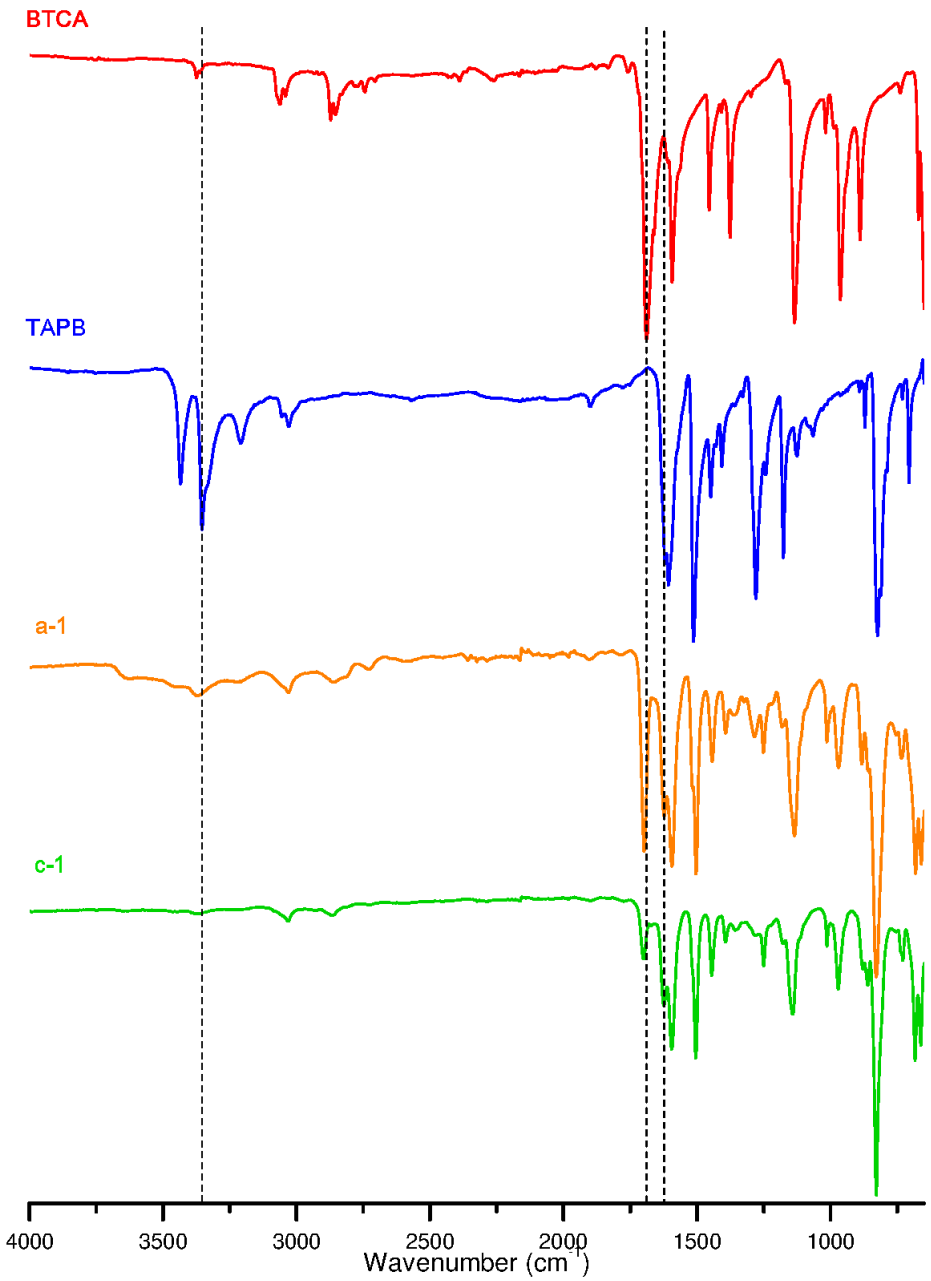

Figure S2. (Top) Solid-state ^{13}C CP-MAS NMR spectra of **a-1** (top), and **c-1** (bottom). Asterisks denote spinning sidebands. (Below) Representation of the imine-based structure and the corresponding assignment of the ^{13}C CP-MAS NMR peaks.

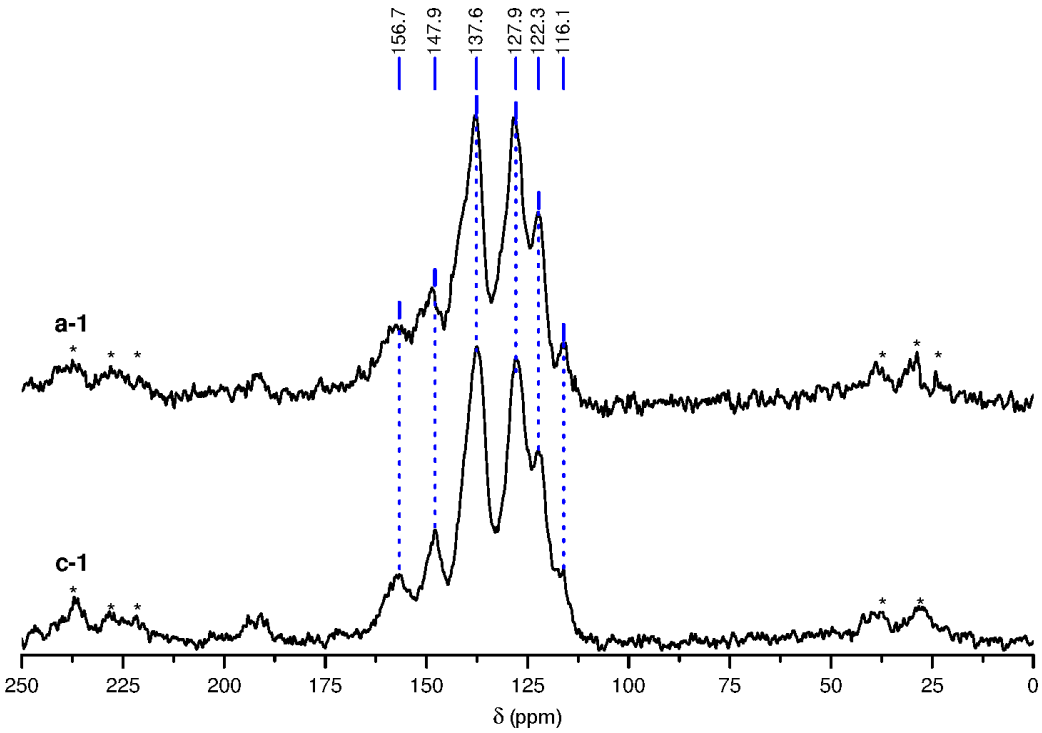

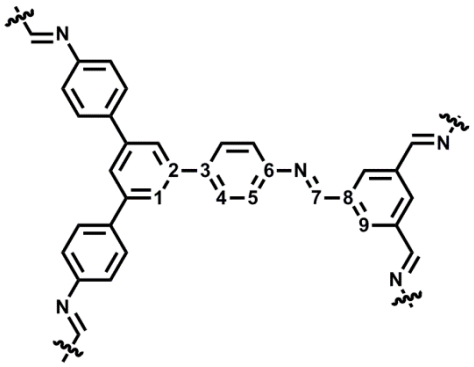

Signal (ppm)	Assignment
156.7	7
147.9	6
137.6	2, 3, 8
127.9	4, 9
122.3	1
116.1	5

Figure S3. TGA trace for **a-1**.

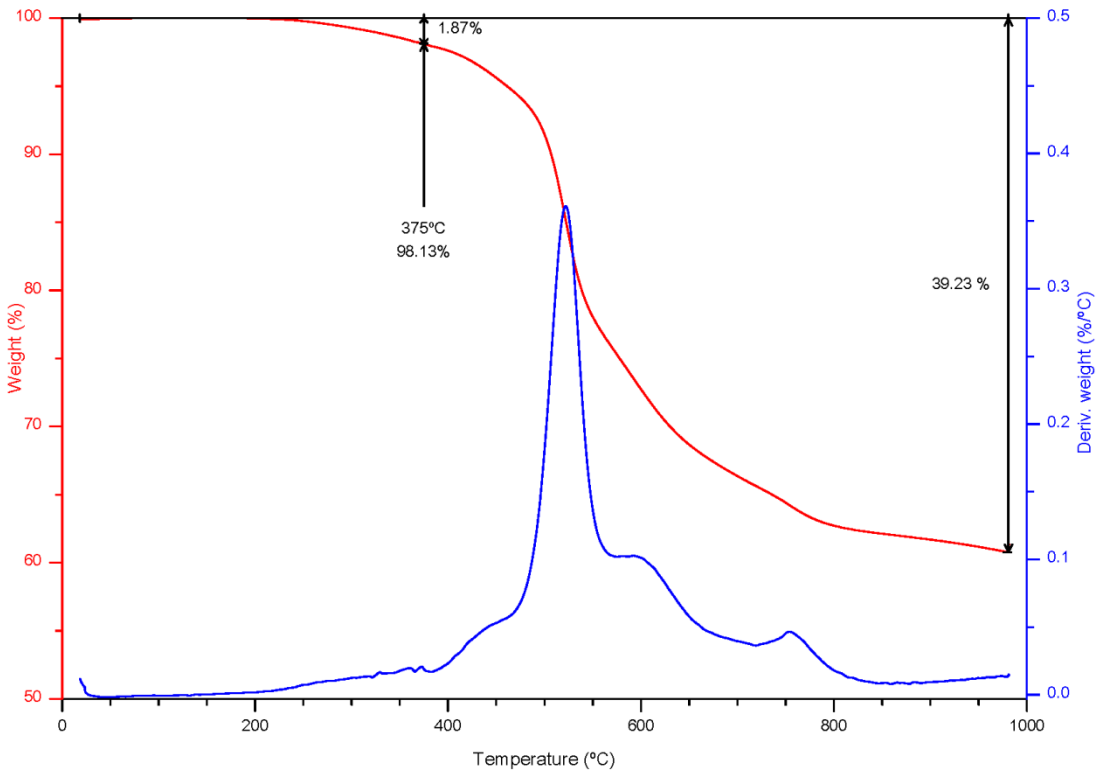

Figure S4. TGA trace for **c -1**.

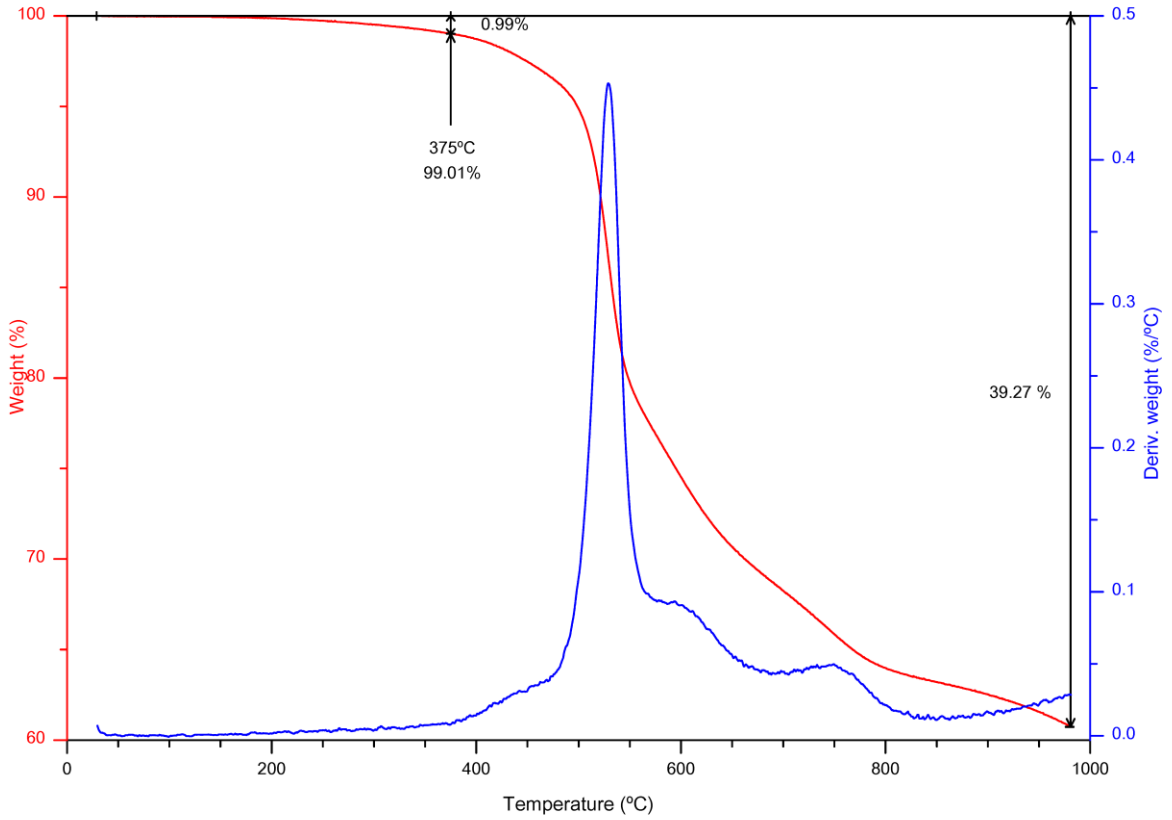

Figure S5. Dynamic Light Scattering (DLS) measurements of an aqueous colloidal solution of (a) **a-1** and (b) **c-1**.

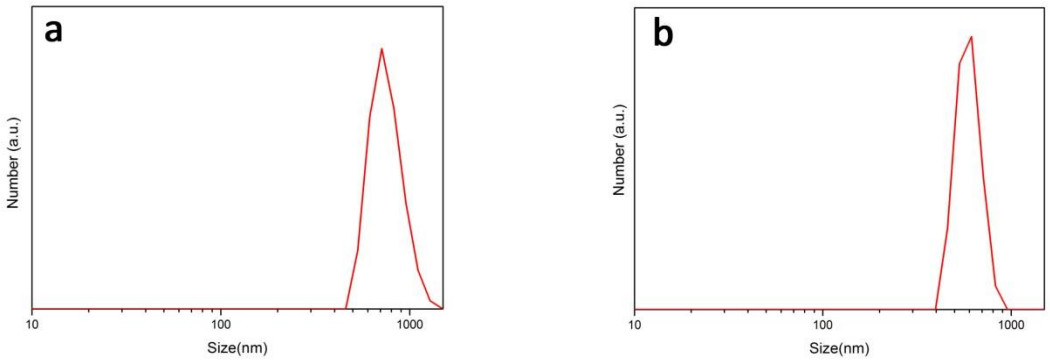

Figure S6. Comparison of calculated PXRD diagram of the staggered (green) and eclipsed (red) COF with experimental PXRD diagram of **c -1** (black).

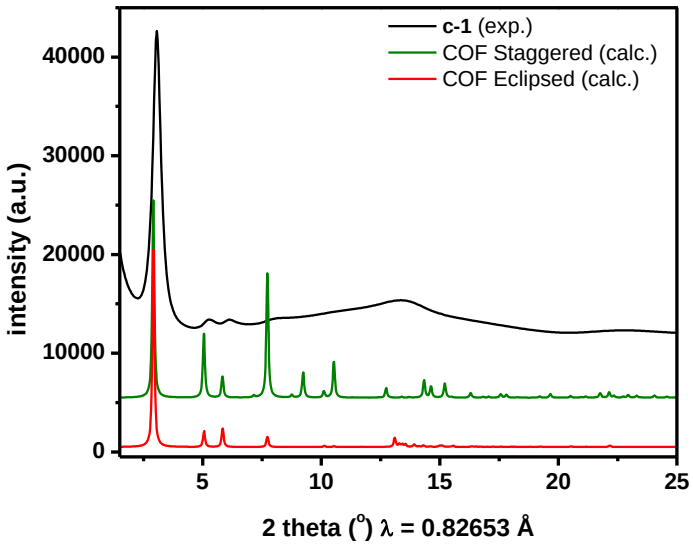

Figure S7. BET plot for N_2 sorption in **a-1**.

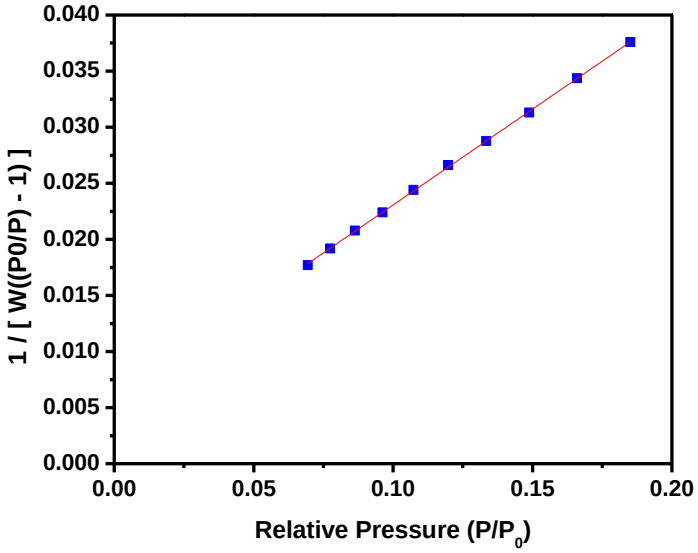

BET surface area: 24.6012 ± 0.1231 m^2/g
Slope: 0.170959 ± 0.000878 g/cm^3 STP
Y-intercept: 0.005966 ± 0.000109 g/cm^3 STP
C: 29.655030
Qm: 5.6521 cm^3/g STP
Correlation coefficient: 0.9998944
Molecular cross-sectional area: 0.1620 nm^2

Figure S8. BET plot for N_2 sorption in the 2 h-treated **a-1**.

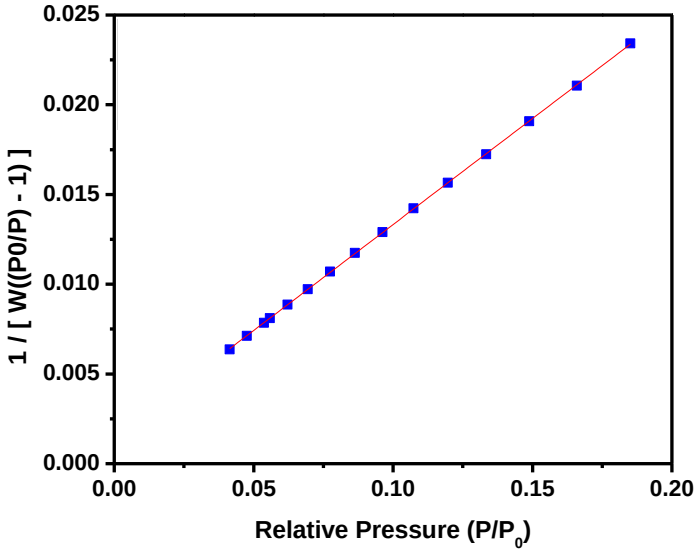

BET surface area: 36.3728 ± 0.0568 m²/g
Slope: 0.118157 ± 0.000186 g/cm³ STP
Y-intercept: 0.001509 ± 0.000020 g/cm³ STP
C: 79.312496
Qm: 8.3566 cm³/g STP
Correlation coefficient: 0.9999839
Molecular cross-sectional area: 0.1620 nm²

Figure S9. BET plot for N_2 sorption in the 12 h-treated **a-1**.

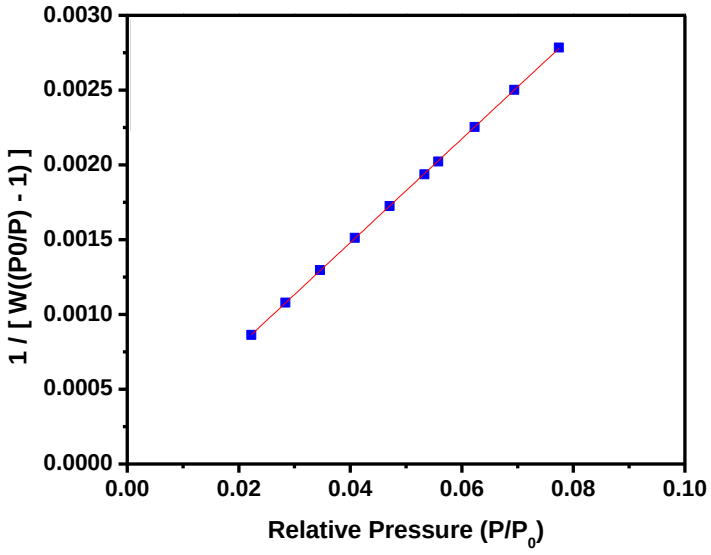

BET surface area: 125.0931 ± 0.2662 m²/g
Slope: 0.034702 ± 0.000074 g/cm³ STP
Y-intercept: 0.000092 ± 0.000004 g/cm³ STP
C: 377.146553
Qm: 28.7400 cm³/g STP
Correlation coefficient: 0.9999818
Molecular cross-sectional area: 0.1620 nm²

Figure S10. BET plot for N_2 sorption in the 24 h-treated **a-1**.

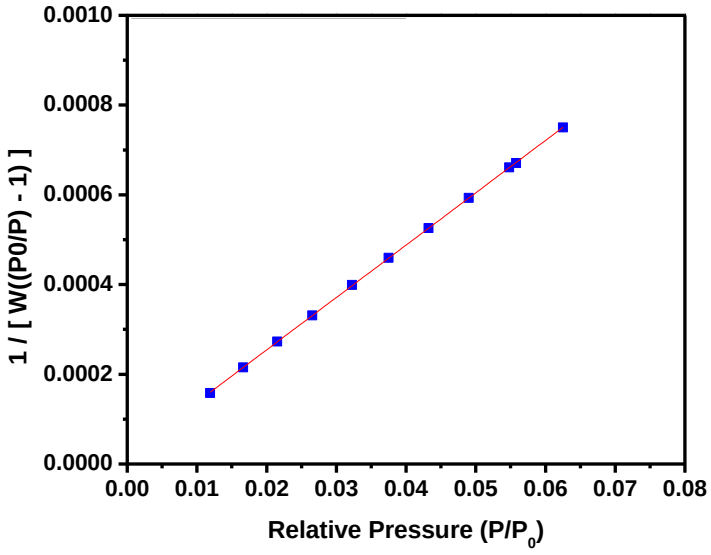

BET surface area: 372.3449 ± 0.5171 m^2/g
Slope: 0.011669 ± 0.000016 g/cm^3 STP
Y-intercept: 0.000021 ± 0.000001 g/cm^3 STP
C: 554.396981
Qm: 85.5458 cm^3/g STP
Correlation coefficient: 0.9999913
Molecular cross-sectional area: 0.1620 nm^2

Figure S11. BET plot for N_2 sorption in the 48 h-treated **a-1**.

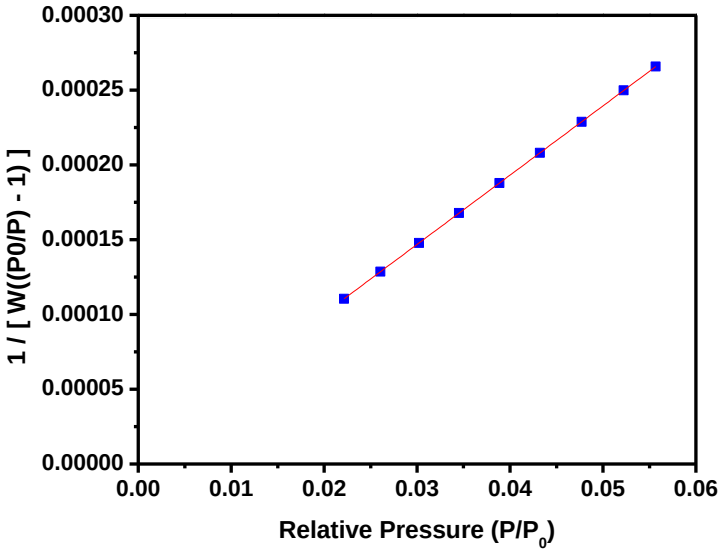

BET surface area: 938.3967 ± 0.3102 m²/g
Slope: 0.004630 ± 0.000002 g/cm³ STP
Y-intercept: 0.000008 ± 0.000000 g/cm³ STP
C: 585.016261
Qm: 215.5956 cm³/g STP
Correlation coefficient: 0.9999996
Molecular cross-sectional area: 0.1620 nm²

Figure S12. BET plot for N_2 sorption in **c-1** (168 h-treated).

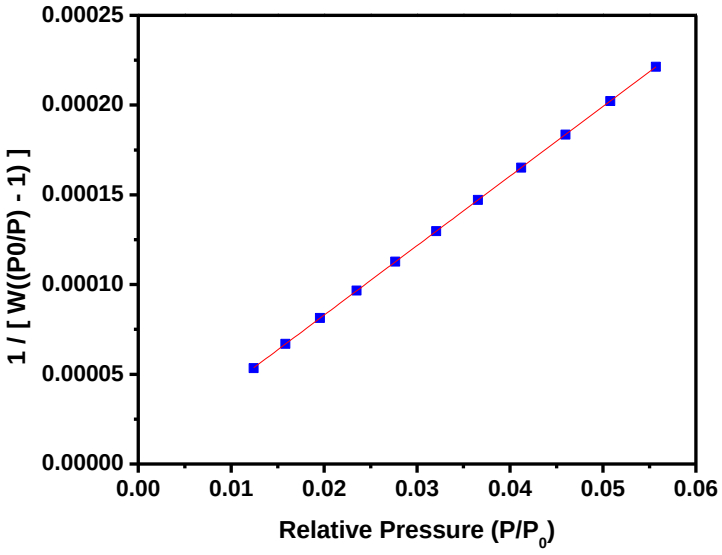

BET surface area: 1121.6708 ± 0.7206 m²/g
Slope: 0.003875 ± 0.000002 g/cm³ STP
Y-intercept: 0.000005 ± 0.000000 g/cm³ STP
C: 709.057482
Qm: 257.7026 cm³/g STP
Correlation coefficient: 0.9999981
Molecular cross-sectional area: 0.1620 nm²

Figure S13. CO_2 sorption isotherms collected at 203 K, 258 K, 273 K, 288 K and 298 K for **a-1** (left) and **c-1** (right).

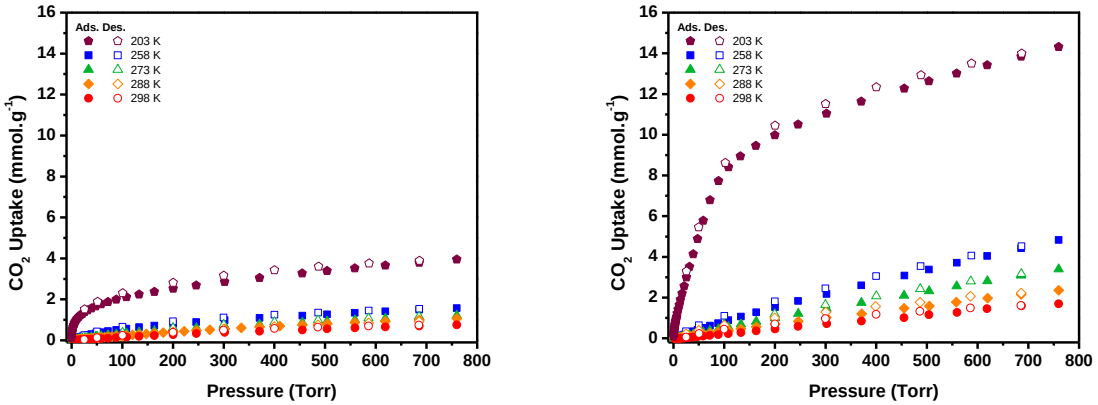

Figure S14. Heats of adsorption of CO_2 for **a-1** (left), calculated from the isotherms derived from CO_2 adsorption isotherms collected at 258 K, 273 K, 288 K and 298 K (right).

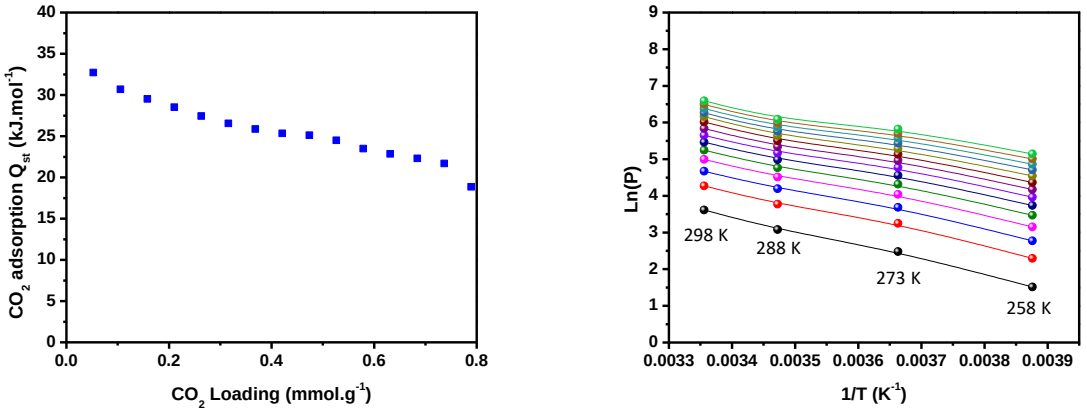

Figure S15. Heats of adsorption of CO_2 for **c-1** (left), calculated from the isotherms derived from CO_2 adsorption isotherms collected at 258 K, 273 K and 298 K (right).

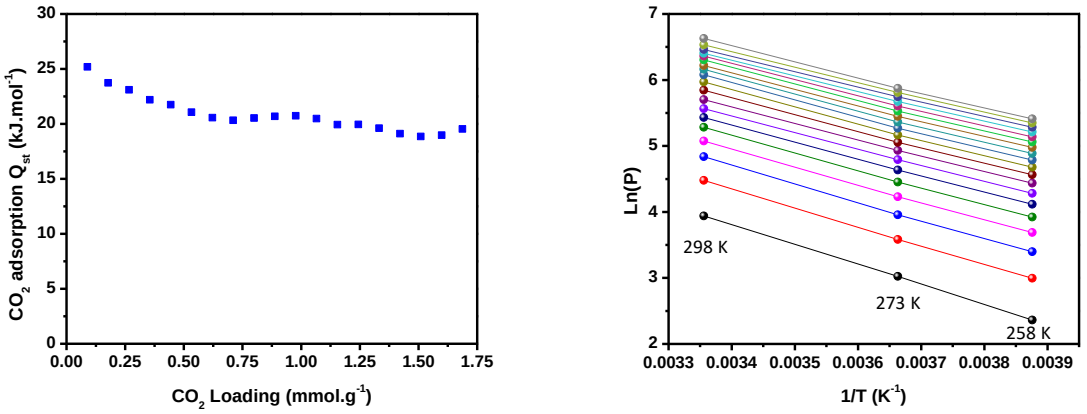

Figure S16. HAADF-STEM images of (a) **Fe_3O_4@a-1** and (b) **Fe_3O_4@c-1**. Scale bars are 200 nm.

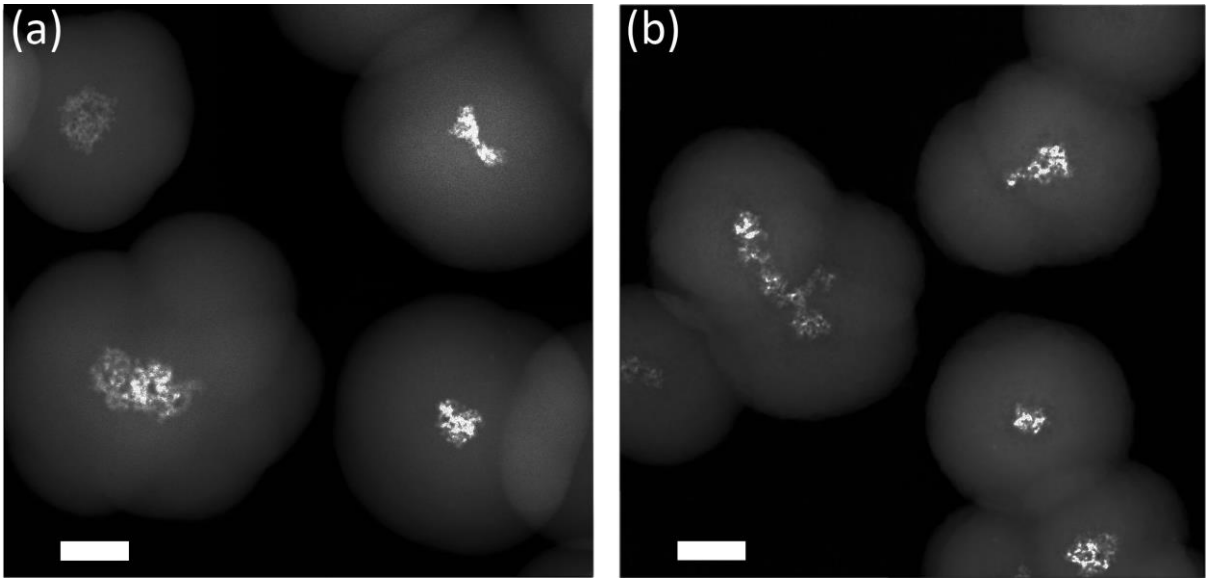

Figure S17. Comparison of calculated PXRD diagram of **c-1** (red) and experimental PXRD diagram of Fe_3O_4 NPs (blue) with **Fe_3O_4@c-1** (black).

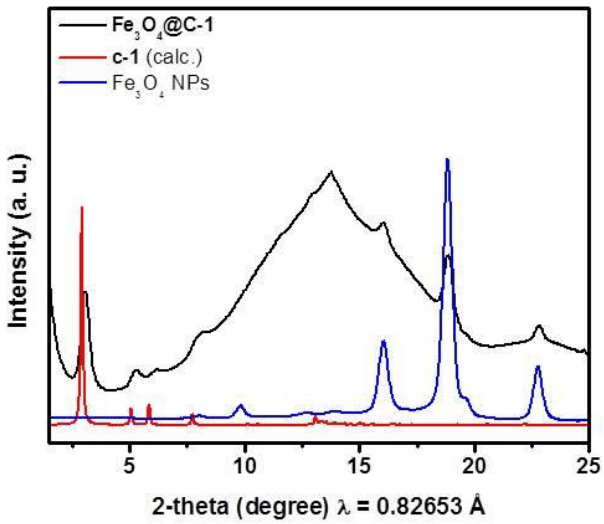

Figure S18. EDX of **Fe_3O_4@c-1**.

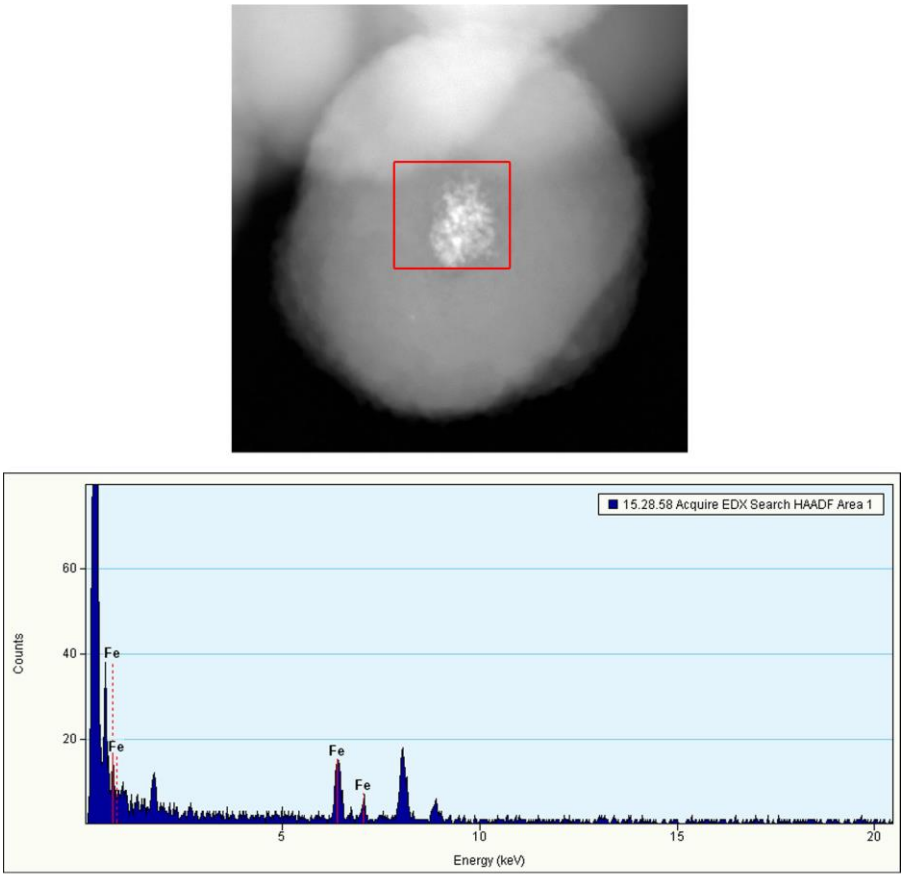

Figure S19. Comparison of calculated PXRD diagram of **c-1** (red) and Au NPs (blue) with experimental PXRD diagram of **Au@c-1** (black).

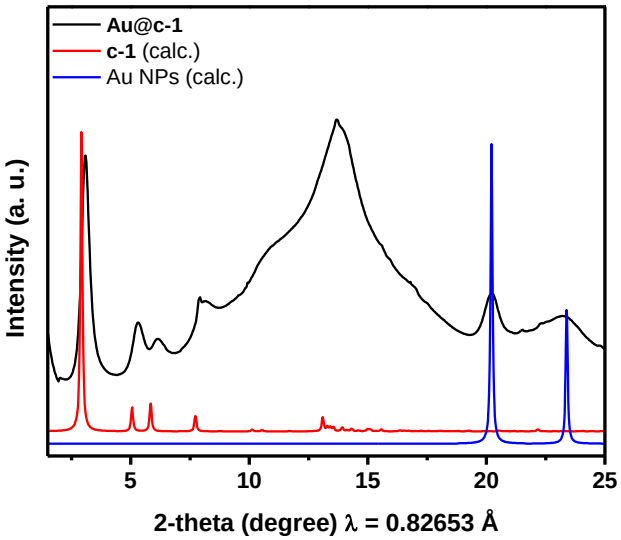

Figure S20. EDX of **Au@c-1**.

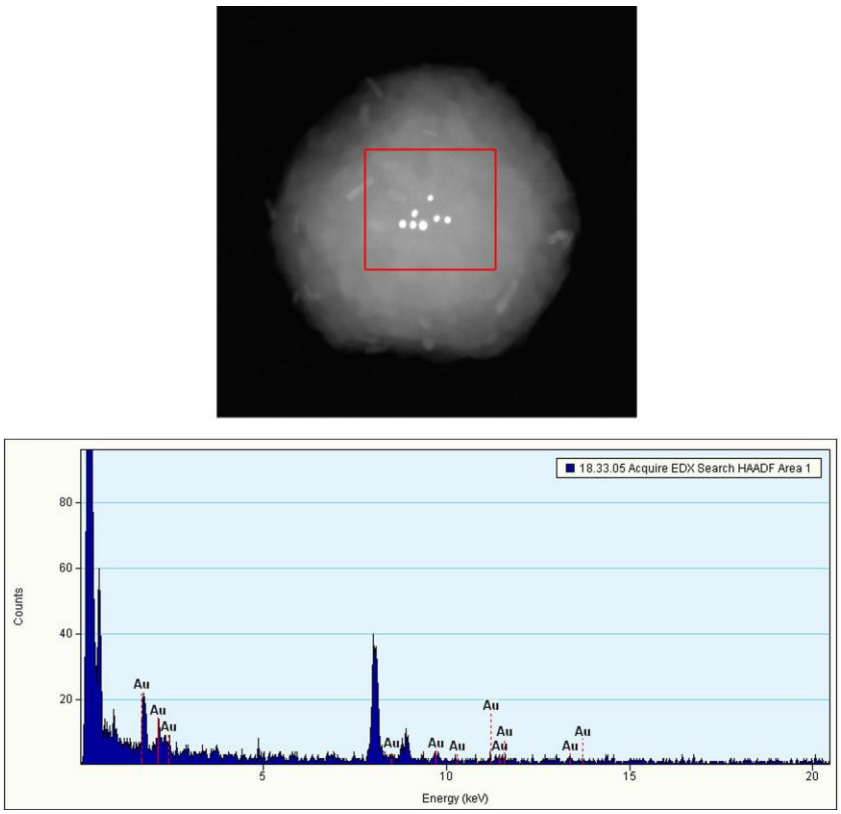

Figure S21. Comparison of calculated PXRD diagram of **c-1** (red) and Pd NPs (blue) with experimental PXRD diagram of **Pd@c-1** (black).

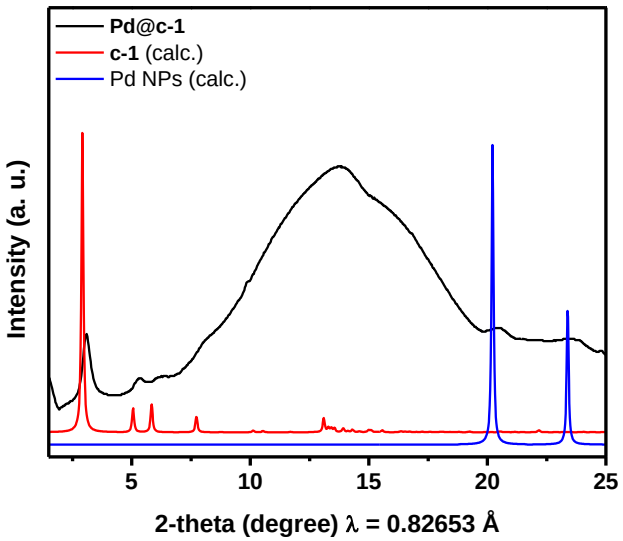

Figure S22. EDX of (a) **Pd@c-1**.

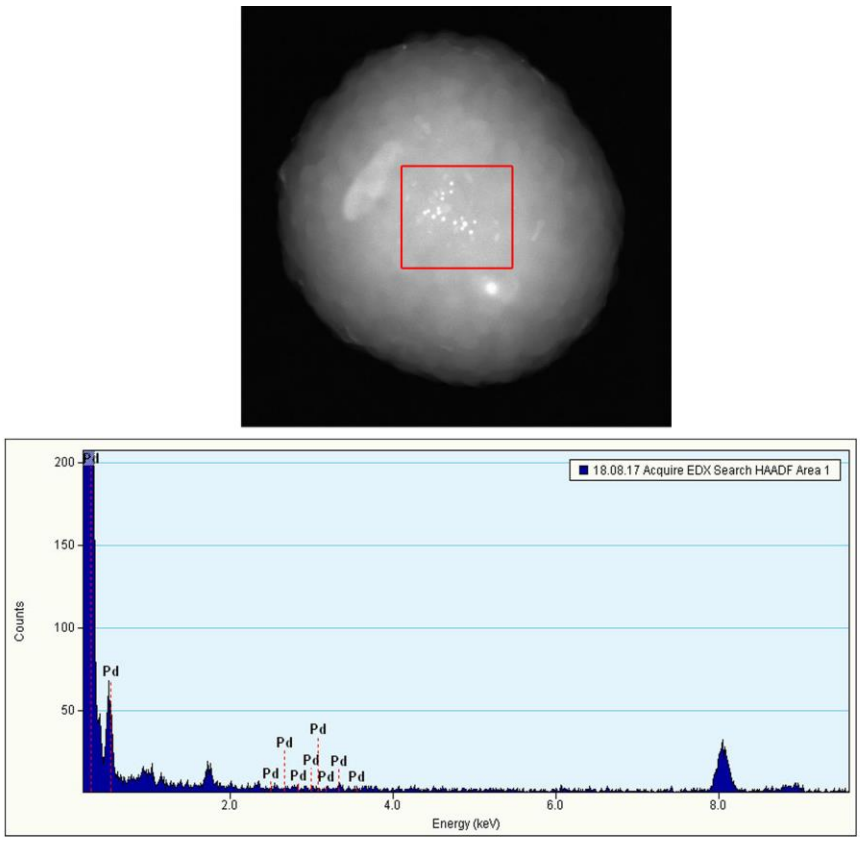

Figure S23. Scanning electron microscopy (SEM) and HAADF-STEM images of (a,b) **Pd@c-1** and (c,d) **Au@c-1** after 4-NP reduction.

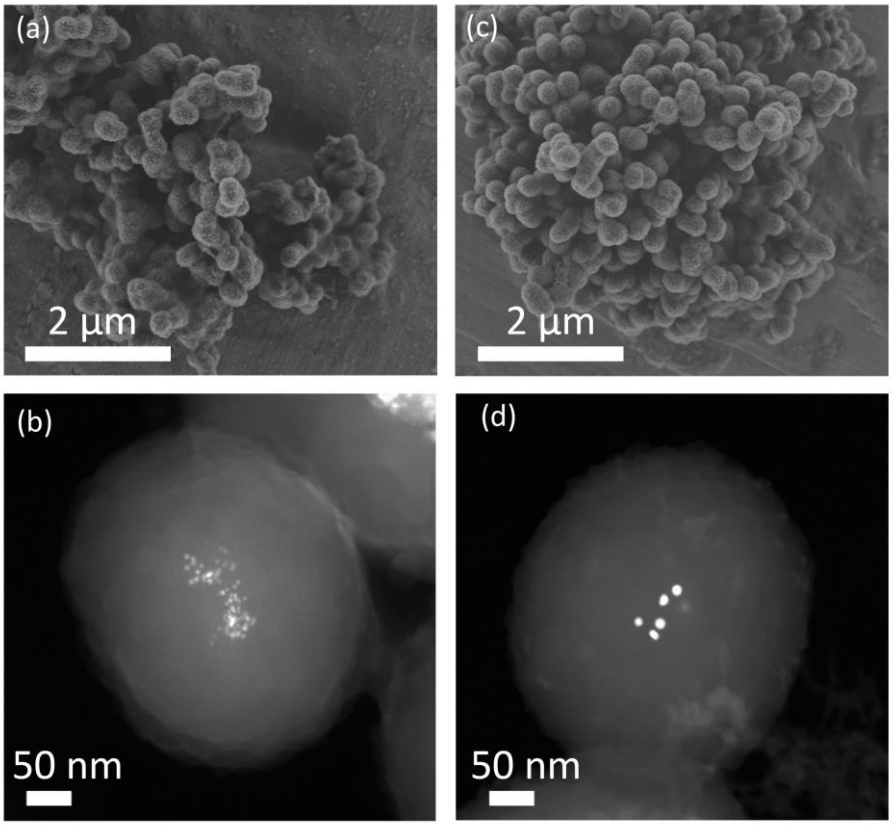

Figure S24. Reduction of *4-NP* in presence of **c-1** after 16 min of treatment.

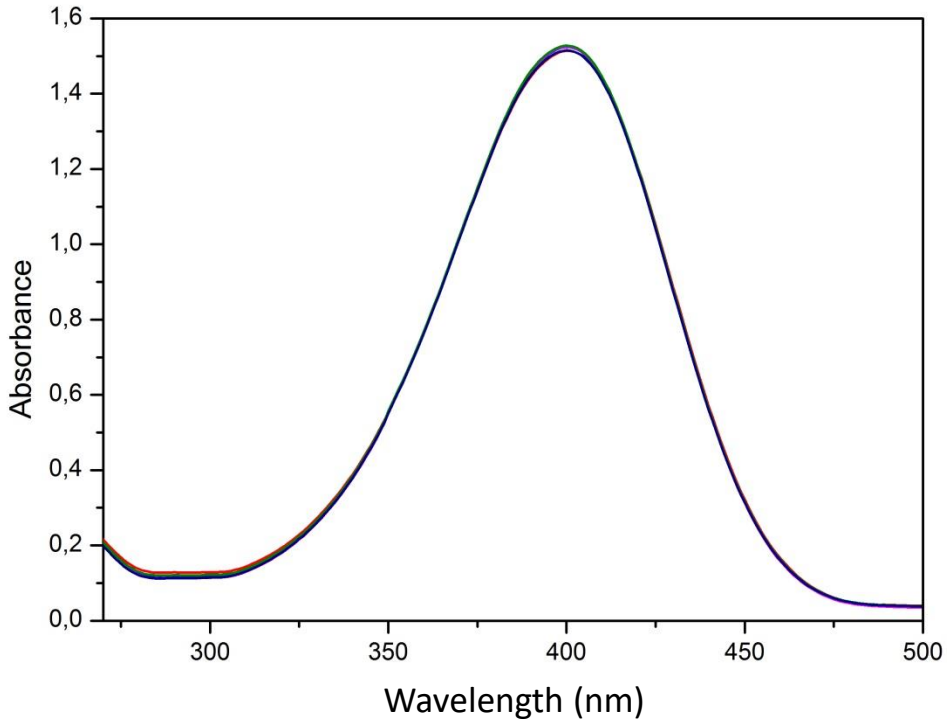

REFERENCES

[1] A. D. Ruigomez, D. Rodriguez-San-Miguel, K. C. Stylianou, M. Cavallini, D. Gentili, F. Liscio, S. Milita, O. M. Roscioni, M. L. Ruiz-Gonzalez, C. Carbonell, D. Maspoch, R. Mas-Balleste, J. L. Segura, F. Zamora, *Chem-Eur J* **2015**, *21*, 10666-10670.

[2] J. Juanhuix, F. Gil-Ortiz, G. Cuni, C. Colldelram, J. Nicolas, J. Lidon, E. Boter, C. Ruget, S. Ferrer, J. Benach, *J. Sync. Rad.* **2014**, *21*, 679-689.

[3] A. P. Hammersley, *ESRF Intern. Rep.* **1997**, *ESRF97HA02T*, "FIT2D: An Introduction and Overview".

[4] F. Rouquerol, J. Rouquerol, K. Sing, *Adsorption by Powders & Porous Solids: Principles, Methodology and Applications*, Academic Press, London, **1999**.

[5] N. G. Bastús, J. Comenge, V. Puntes, *Langmuir* **2011**, *27*, 11098-11105.

[6] X. Liu, Z. Ma, J. Xing, H. Liu, *J. Mag. Mag. Mater* **2004**, *270*, 1-6.